miR-379 inhibits cell proliferation and epithelial-mesenchymal transition by targeting CHUK through the NF-κB pathway in non-small cell lung cancer

BIN LIU[1*], ZHENG WANG[2*], SHIZHAO CHENG[2*], LIN DU[2], YAN YIN[2], ZHEN YANG[3] and JINGMIN ZHOU[1]

Departments of [1]Respiratory and Critical Care Medicine, and [2]Thoracic Surgery, Tianjin Chest Hospital, Tianjin 300000; [3]Department of Pathogen Biology, Basic Medical School, Tianjin Medical University, Tianjin 300070, P.R. China

Received June 1, 2018; Accepted March 29, 2019

DOI: 10.3892/mmr.2019.10362

Abstract. An increasing body of evidence has demonstrated that microRNA (miR) deregulation serves pivotal roles in tumor progression and metastasis. However, the function of miR-379 in lung cancer remains understudied, particularly in non-small cell lung cancer (NSCLC). Bioinformatics and luciferase reporter analyses confirmed that conserved helix-loop-helix ubiquitous kinase (CHUK) is a target of miR-379, which may directly bind to the 3'-untranslated region of CHUK and significantly downregulate its expression in NSCLC cells. Transwell assays were used to evaluate the role of miR-379 in cell migration and invasion, and western blotting was used to address the association between miR-379 and epithelial-mesenchymal markers, including E-cadherin, cytokeratin and Vimentin. In the present study, miR-379 expression in NSCLC tissues and cell lines was downregulated, which may be associated with the poor survival of patients with NSCLC. miR-379 may act as a tumor suppressor in NSCLC, potentially by suppressing cell growth and proliferation, delaying G1-S transition, enhancing cell apoptosis and suppressing NSCLC cell migration and invasion. Furthermore, it was also observed that CHUK may function as an oncogene, and downregulation of CHUK induced by miR-379 may partially rescue the malignant characteristics of tumors, indicating that miR-379 may be suppressed in tumorigenesis. The overexpression of miR-379 may prevent the growth of NSCLC tumors via CHUK suppression and the downstream nuclear factor-κB pathway. The results of the present study demonstrated that miR-379 may act as a tumor suppressor, and may constitute a potential biomarker and a promising therapeutic agent for the treatment for NSCLC.

Correspondence to: Dr Jingmin Zhou, Department of Respiratory and Critical Care Medicine, Tianjin Chest Hospital, 261 Taierzhuang South Road, Jinnan, Tianjin 300000, P.R. China
E-mail: zhou_560425@aliyun.com

*Contributed equally

Key words: microRNA-379, non-small cell lung cancer, nuclear factor-κB, signaling pathway, conserved helix-loop-helix ubiquitous kinase

Introduction

Lung cancer, the most common of malignant tumors, is a leading cause of cancer-associated mortality all over the world (1). There are two main types of lung cancer: Non-small cell lung cancer (NSCLC) and SCLC (2). NSCLC is the most common type, corresponding to 85% of all lung cancer cases (3). Approximately two-thirds of patients diagnosed with NSCLC present the pathology of an already advanced stage (4). Although new drugs have been developed, including epidermal growth factor receptor and anaplastic lymphoma kinase inhibitors, due to early tumor recurrence and metastasis, the overall survival of patients with NSCLC remains poor (5). Therefore, it is essential to find novel biomarkers that can precisely predict the prognosis of patients diagnosed with NSCLC, and to discover new targets that may help treat this disease more effectively.

MicroRNAs (miRs/miRNAs) are small non-coding RNAs (~18-25 nucleotides) that negatively regulate gene expression at the post-transcriptional level by inhibiting mRNA translation or causing its degradation, all via complementarities with the 3'-untranslated region (UTR) of their target genes (6,7). The expression of miRs in tumor and normal tissues is known to be different, a fact that has been described in a number of different tumors (8). A previous study has demonstrated that miRs are involved in the regulation of a number of processes, including cell proliferation, metabolism, differentiation and apoptosis (9). Further research has confirmed that miRs also serve a pivotal role in the onset and progression of cancer (9,10). Other studies have demonstrated that multiple miRs are up-or downregulated in NSCLC (11-13). For example, Wang *et al* (14) reported that miR-124 suppresses cell viability and enhances cell apoptosis by inhibiting signal transducer and activator of transcription 3 in NSCLC. In addition, Liu *et al* (15) reported that the downregulation of miR-335 promotes cell viability or inhibits cell apoptosis via the upregulation of transformer 2β homolog, mediated by the activation of the protein kinase B (AKT) signaling

pathway in A459 lung cancer cells. Xue *et al* (16) reported that miR-342-3p inhibits cell proliferation and migration, and enhances cell apoptosis in NSCLC cells by targeting anterior gradient 2. Regarding miR-379, according to PubMed (www.ncbi.nlm.nih.gov/pubmed/) only six studies have evaluated its association with lung cancer, and the mechanism of miR-379 regulation in NSCLC remains unreported.

In the present study, miR-379 was observed to be downregulated in NSCLC cell lines and tissues. Functional analyses and experiments demonstrated that upregulation of miR-379 significantly suppressed proliferation, migration, invasiveness and the epithelial-mesenchymal transition (EMT) process of NSCLC cells. In addition, Transwell migration assays revealed that the overexpression of miR-379 inhibited NSCLC cell migration and invasion. Furthermore, conserved helix-loop-helix ubiquitous kinase (CHUK), formally termed inhibitor of nuclear factor-κB (NF-κB) kinase subunit α (IKKα) was confirmed to be a target of miR-379 and that it has an oncogenic role in NSCLC progression via the activation of the NF-κB signaling pathway. These results indicated that miR-379 may inhibit NSCLC progression by directly targeting CHUK and by activating the NF-κB signaling pathway.

Materials and methods

Patient tissue samples. A total of 30 pairs of human NSCLC and matched normal tissues were obtained from 30 patients admitted to the Department of Respiratory and Critical Care Medicine, Tianjin Chest Hospital (Tianjin, China). All of the human NSCLC and matched normal tissues were pathologically and histologically evaluated. All samples were stored in liquid nitrogen before use. The present study followed the guidelines of The Declaration of Helsinki. All participants provided written informed consent, and the present study was approved by the Ethical Oversight Committee of Department of Respiratory and Critical Care Medicine, Tianjin Chest Hospital (Tianjin, China).

Cell culture. The NSCLC cell lines, namely H1993 (NCI-H1993), H1650 (NCI-H1650), H1299 (NCI-H1299), A549 (A-549) and SK-MES-1, and a non-tumorigenic human bronchial epithelial cell line (BEAS-2B) were purchased from American Type Culture Collection. These were cultured in Dulbecco's modified Eagle's medium (DMEM; HyClone; GE Healthcare Life Sciences) containing 10% fetal bovine serum (FBS; HyClone; GE Healthcare Life Sciences), streptomycin (100 μg/ml) and penicillin (100 μg/ml), and maintained in a humidified atmosphere at 37˚C with 5% CO_2.

Cytosolic and nuclear protein isolation. A549 and H1993 cells ($1x10^7$ cells/ml) were harvested, washed with PBS, centrifuged (900 x g, for 6 min, at room temperature), and re-suspended in ice-cold buffer A [10 mM HEPES (pH 7.0), 1.5 mM $MgCl_2$, 10 mM KCl, 0.5 mM DTT and 0.2 mM PMSF]. After 10 min of incubation on ice, the cells were centrifuged again (900 x g, for 6 min, at room temperature), and the supernatant (cytosolic fraction) was stored at -80˚C. The pellet containing the nuclear fraction was re-suspended in buffer C [20 mM HEPES (pH 7.9), 20% glycerol, 420 mM NaCl, 1.5 mM $MgCl_2$, 0.2 mM EDTA, 0.5 mM DTT and 0.2 mM PMSF], and incubated for 20 min at 0˚C. Following vortex mixing, the resulting suspension was centrifuged at 1,000 x g for 10 min at 4˚C, and the supernatant (nuclear extract) was stored at -80˚C. The protein concentration of both the cytosolic and nuclear extracts was determined using the Bradford method via the Bio-Rad protein assay kit (Bio-Rad Laboratories, Inc.).

Plasmid construction. The potential targets of miR-379 were predicted using miRNA.org (http://www.microrna.org/microrna/home.do), TargetScan 7.1 (http://www.targetscan.org/vert_71/), miRbase (http://www.mirbase.org/index.shtml) and miRanda (http://www.mirdb.org/). The miRBase Targets version 2.0 (http://www.mirbase.org/index.shtml) was used to search for the potential miR-379 target sites in the CHUK 3'UTR.

The 3'UTR fragment of the CHUK gene containing the predicted miR-3379 binding site was amplified by PCR from the A549 cell RNA. Total RNA was isolated from A549 cell using TRIzol® (Invitrogen; Thermo Fisher Scientific, Inc.), according to the manufacturer's instructions. RNA (1 mg) was reverse transcribed into cDNA using the Omniscript RT kit (Qiagen GmbH), according to the manufacturer's protocol. The temperature protocol for reverse transcription was as follows: 37˚C for 60 min, followed by a final step of 37˚C for 5 sec. pCHUK, pSilencer, short hairpin RNA CHUK (shR-CHUK), pri-miR-379, ASO-miR-379, pcDNA3 and ASO-NC (Shanghai Jierui Biological Engineering Co., Ltd.) represent overexpressed CHUK, empty vector, knockdown CHUK, overexpressed miR-379, knockdown miR-379, empty vector and empty vector, respectively. The sequences of the primers used in plasmid construction were as follows: pCHUK forward, 5'-GTACCAGCATCGGGAACTTG-3', and pCHUK reverse, 5'-ATGGCACCATCGTTCTCTGT-3'; shR-CHUK forward, 5'-GATCCGCAGTGCACTATGTGTCTGTTCAAG AGACAGACACATAGTGCACTGCTTTTTTGGAAA-3', and shR-CHUK reverse, 5'-AGCTTTTCCAAAAAAGCAGTG CACTATGTGTCTGTCTCTTGAACAGACACATAGTGC ACTGCG-3'; pri-miR-379 forward, 5'-CGGGGTACCGGTATA AGGCAGGGACTGGG-3', and pri-miR-379 reverse, 5'-CCG GAATTCGGATATGTGGGACCCGAAGG-3'; ASO-miR-379 forward, 5'-CACUGGUACAAGGGUUGGGAGA-3', and ASO-miR-379 reverse, 5'-CAGUACUUUUGUGUAGUA CAA-3'. The thermocycling conditions of the PCR amplification conditions were as follows: 95˚C for 40 sec and 40 cycles of 95˚C for 5 sec, 60˚C for 40 sec, and finally extend for 72˚C 5 min.

For the luciferase assay, the sequence inserted into the *Bam*HI and *Eco*RI sites of the pcDNA3/enhanced green fluorescent protein (EGFP) vector (Promega Corporation) were immediately downstream from the stop codon of EGFP. The resulting vector was named CHUK-3'UTR. A mutant version (CHUK-3'UTR mut) with alterations in the seed sequence of the miR-379 binding site was also constructed using the same PCR method (CHUK-3'UTR mut forward, 5'-CGC GGATCCCCTCAAAATAAAGAAGTATGGTAAT-3', and CHUK-3'UTR mut reverse, 5'-CCGGAATTCAGCTTT TTTATTTGTTAATGTCACA-3'). All the insertions were confirmed upon sequencing.

Transfection assay. The pri-miR-379 or antisense oligonucleotide (ASO)-miR-379 and respective controls [pcDNA3 and ASO-negative control (NC)] were transfected into human

NSCLC cell lines using Lipofectamine™ 2000 (Thermo Fisher Scientific, Inc.), according to the manufacturer's protocol. A total of 100 nM miR-17-3P mimic, inhibitor or negative control miRNA (Guangzhou RiboBio Co., Ltd.) were transfected into cultured cells in accord with manufacturer's instructions. After 48 h, the transfection efficacy was evaluated by reverse transcription-quantitative PCR. The miR-379 expression vector (pri-miR-379) was amplified from genomic DNA and cloned into the pcDNA3 vector at *Kpn*I and *Eco*RI sites. The 2'-O-methyl-modified miR-379 antisense oligo nucleotide (ASO-miR-379) was commercially synthesized as an inhibitor of miR-379.

RT-qPCR analysis. Total RNA and miR were isolated from cells or frozen tissues with TRIzol® (Invitrogen; Thermo Fisher Scientific, Inc.) and cDNA was synthesized with the miRVana miR Isolation kit (Ambion; Thermo Fisher Scientific, Inc.) and PrimeScript RT Master Mix (Takara Biotechnology Co., Ltd., Dalian, China) according to the manufacturer's protocol. The temperature protocol for the reverse transcription was as follows: 37˚C for 60 min, followed by a final step of 37˚C for 5 sec. The qPCR was used to assay the expression levels of CHUK (forward, 5'-TGGAGCCCCTGAAGAAGAG-3', and reverse, 5'-AAGTGCGTTGTGCGGTAGC-3'), NFKB1A (forward, 5'-CTGCTCTCCCTTCCTCAGAC-3', and reverse, 5'-TGAGGTAGGACCAGGAAACC-3'), β-actin (forward 5'-TAGTTGCGTTACACCCTTTCTTG-3', and reverse, 5'-GCTGTCACCTTCACCGTTCC-3'), miRNA-379 (forward, 5'-GCGCTTATTGCTTAAGAATAC-3', and reverse, 5'-CAG TGCAGGGTCCGAGGT-3') and U6 (forward, 5'-GCTTCG GCAGCACATATACTAAAAT-3', and reverse, 5'-CGCTTC ACGAATTTGCGTGTCAT-3)'. These were performed on an ABI7300 Real-Time PCR System (Applied Biosystems; Thermo Fisher Scientific, Inc.) using the SYBR® Green PCR Master Mix (Thermo Fisher Scientific, Inc.) and a Bio-Rad CFX-96 RT-PCR system (Bio-Rad Laboratories, Inc.), according to the manufacturer's instructions. The thermocycling conditions were as follows: Preliminary denaturation at 96˚C for 2 min, followed by 40 cycles of denaturation at 96˚C for 15 sec, annealing at 60˚C for 1 min and elongation at 60˚C for 1 min. miR-379 levels were detected using a miR-specific TaqMan MicroRNA Assays kit (Applied Biosystems, Thermo Fisher Scientific, Inc.) according to the manufacturer's instructions. The thermocycling conditions were: 95˚C for 10 min; 40 cycles of 95˚C for 1 min, 63˚C for 2 min, 72˚C for 1 min; final 72˚C for 10 min. The relative expression levels of each gene were calculated and normalized using the $2^{-\Delta\Delta Cq}$ method relative to U6 or β-actin (17). All the reactions were run in triplicate.

Cellular proliferation and colony formation. An MTT assay was used to determine the cell viability. Cells were seeded 24 h after transfection was completed. A total of $2x10^3$ cells were seeded in a total volume of 100 µl in 96-well plates. The MTT assay was performed at 24, 48 and 72 h, and DMSO was used to dissolve the formazan and stop the reaction. The optical density was measured using a Quant Universal Microplate Spectrophotometer (BioTek Instruments, Inc.) at 490 nm.

For the colony formation assay, H1993 and A549 cells (300 cells/well in 12-well plates) were seeded in complete medium (containing DMEM, 10% fetal bovine serum, 100 µg/ml streptomycin and 100 µg/ml penicillin) for 12 days, at 37˚C, with 5% CO_2. Cells were fixed with 4% paraformaldehyde in PBS for 10 min at room temperature, and stained with 0.1% crystal violet for 30 min at room temperature. Only colonies containing >50 cells were counted.

EGFP reporter assay. An EGFP reporter assay was performed to determine the binding of miR-379 to the 3'UTR of CHUK mRNA. A549 and H1993 cells were co-transfected with pri-miR-379, ASO-miR-379 or their respective control vectors and 3'UTR CHUK or 3'UTR CHUK mut, performed as aforementioned. Following transfection in 48-well plates, cells were cultured for 48 h at 37˚C. Firefly and *Renilla* luciferase activities were determined with the Dual-Luciferase Reporter Assay System in a GloMax96 luminescence reader (both from Promega Corporation), according to the manufacturer's instructions. Relative luciferase activity was expressed as the ratio of firefly luciferase activity to the *Renilla* luciferase activity in each sample. High EGFP intensity indicated enhanced promoter activity, reflecting the binding of the UTR to the promoter.

Flow cytometry. A549 and H1993 cells were detached 48 h after transfection. Cells were subsequently washed and fixed with PBS and 75% ethanol at 4˚C overnight. A549 and H1993 cells were washed with PBS after fixation, and treated with propidium iodide stain (Beyotime Institute of Biotechnology) for 30 min at room temperature or Annexin V-FITC (Sigma-Aldrich; Merck KGaA), according to manufacturer's instructions. The cell cycle stage and the levels of apoptosis of both cell types were analyzed with the BD FACSCanto™ II flow cytometry system (BD Biosciences) and the ModFit LT software package (version 3.1; Becton, Dickinson and Company).

Transwell migration and invasion assays. After 24 h from transfection with the associated plasmids, A549 and H1993 were collected and re-suspended in serum-free DMEM. A total of $6x10^5$ cells/ml were added to the upper Transwell chamber inserts, with or without matrix, and the lower Transwell chamber was filled with DMEM supplemented with 20% FBS. Cells were incubated at 37˚C for 48 h. The cells in the lower chamber were fixed with 4% paraformaldehyde in PBS for 10 min at room temperature, and stained with 0.1% crystal violet for 30 min at room temperature. The capacity of cell migration and invasion were determined by measuring the number of cells in the lower chamber under bright-field microscopy (magnification, x200).

Immunofluorescence. Immunochemical staining was performed following the manufacturer's instructions. Briefly, $5x10^3$ cells (A549 and H1993 cells transfected with pcDNA3, pri-miR-379, ASO-NC and ASO-miR-379) were fixed with 4% paraformaldehyde at 37˚C for 30 min, and washed three times with PBS. Cells were washed with PBS containing 0.2% Triton X-100 for 2 min, and incubated with PBS containing 10% donkey serum (HyClone; GE Healthcare Life Sciences) for 30 min, and incubated with a primary antibody against CHUK (1:1,000; cat. no. 2078; Cell Signaling Technology)

overnight at 4˚C. Cells were washed three times with PBS, and then incubated for 60 min at 37˚C in the dark with the corresponding FITC conjugated secondary antibody (1:50; cat no. 9148; Cell Signaling Technology, Inc.). Cells were rinsed three times with PBS, and incubated in the dark with PBS containing DAPI (1:1,000) for 10 min at room temperature to visualize nuclei. A total of five randomly selected fields were then examined at an x200 magnification using a phase contrast fluorescence microscope (Olympus Corporation).

Western blotting. Cells were collected and the total protein content of the transfected and control cells was extracted via lysis using RIPA buffer including protease inhibitor cocktail (Roche Diagnostics GmbH) for 30 min on ice. The total protein concentration was measured with a bicinchoninic acid protein assay before immunoblotting. Protein lysates (50 μg/lane) were separated on a 10% SDS-PAGE and transferred onto polyvinylidene fluoride membranes (EMD Millipore). The membranes were blocked with 5% skimmed milk at room temperature for 1 h. The primary antibodies were used according to the manufacturer's instructions, at 4˚C overnight. The primary antibodies used in the present study were E-cadherin (1:1,000; cat. no. 3195; Cell Signaling Technology, Inc.), cytokeratin (1:2,000; cat no. sc-15367; Santa Cruz Biotechnology, Inc.), Vimentin (1:1,000; cat. no. 5741 Cell Signaling Technology, Inc.), CHUK (IKKa; 1:1,000; cat. no. 2078; Cell Signaling Technology, Inc.), NF-κB1 (P50; 1:1,000; cat no. ab32360; Abcam), RELA (P65; 1:1,000; cat. no. ab16502; Abcam), GAPDH (1:1,000; sc-47724; Santa Cruz Biotechnology, Inc.), Lamin A (1:500; cat. no. sc-517580 Santa Cruz Biotechnology, Inc.), Bcl-2 (1:500; SAB4300340; Sigma-Aldrich; Merck KGaA), Bcl-XL (1:1,000; cat. no. 2764; Cell Signaling Technology, Inc.), Survivin (1:2,000; cat. no. 2808; Cell Signaling Technology, Inc.) and NFKBIA (Iκβα; 1:1,000; cat. no. 4814 Cell Signaling Technology, Inc.). Subsequently, the membrane was incubated with a horseradish peroxidase-conjugated secondary antibody (1:20,000, cat. no. 7074; Cell Signaling Technology, Inc.) for 2 h at room temperature. The blots were visualized using an enhanced chemiluminescent reagent (Hanbio Biotechnology Co., Ltd.). Densitometric analyses of the western blot bands were performed using Gel-Pro Analyzer software version 6.0 (Media Cybernetics, Inc.). GAPDH and Lamin A were used as internal controls. All of the experiments were performed in triplicate.

Statistical analysis. All data reported are presented as the mean ± standard deviation from at least three independent experiments, unless otherwise noted. All statistical analyses were performed using GraphPad PRISM version 5.0 (GraphPad Software, Inc.). Differences between cancer tissues and the matched controls were analyzed using a paired t-test. For comparisons between two treatment groups, a Student's t-test was used. The correlation between CHUK and miR-379 levels was analyzed using linear regression analysis. Multiple groups were compared using one-way analysis of variance, followed by Tukey's post-hoc test for multiple comparisons. Differences between the expression levels of miRNA-379 and different clinicopathological factors were calculated using the χ^2 test. $P<0.05$ was considered to indicate a statistically significant difference.

Results

miR-379 expression is downregulated in NSCLC tissues and cells. In order to confirm the role of miR-379 in human NSCLC, the expression levels of miR-379 were analyzed in 30 paired tumor tissues and adjacent non-cancerous lung tissues by RT-qPCR. The results revealed that the expression of miR-379 was significantly downregulated in human NSCLC tissues compared with adjacent non-cancerous tissue samples (Fig. 1A). miR-379 expression in the human NSCLC cell lines (H1993, H1650, H1299, SK-MES-1 and A549) and BEAS-2B cell line was also evaluated. The miR-379 expression levels were markedly downregulated in the human NSCLC cell lines compared with BEAS-2B (Fig. 1B), which was consistent with the data from the tissue samples (Fig. 1A). These results suggested that miR-379 may be involved in the occurrence of NSCLC.

Upregulation of miR-379 inhibits the proliferation, migration, invasion and EMT process of NSCLC cells. To confirm whether miR-379 affects NSCLC progression, H1993 and A549 cells were transfected with pcDNA3, pri-miR-379, ASO-NC or ASO-miR-379. RT-qPCR assays demonstrated that transfection with pri-miR-379 and ASO-miR-379 led to the up- and downregulation, respectively, of miR-379 in H1993 and A549 cells (Fig. 1C). In addition, as shown in Fig. 1D, A549-ASO-miR-379 cells appeared to be more mesothelial compared with the more epithelial-like A549-ASO-NC cells, indicating that dysregulation of miR-379 may be relevant to tumor metastasis. In addition, the overexpression of miR-379 decreased cell viability, while the knockdown of miR-379 appeared to promote the viability of H1993 and A549 cells by MTT (Fig. 1E). Colony formation assays further corroborated these results, as indicated by the increase and decrease in the colony formation rate following the down- and upregulation, respectively, of miR-379 (Fig. 1F).

To confirm whether miR-379 influences cell migration and invasion, transfection with pri-miR-379 or ASO-miR-379 and its corresponding control were performed. The results revealed that miR-379 overexpression significantly decreased the invasion and migration of H1993 and A549 cells compared with the pcDNA3-NC, and miR-379 knockdown increased the invasion and migration of H1993 and A549 cells compared with the ASO-NC (Fig. 1G). Finally, western blotting was used to assess the levels of EMT markers, including E-cadherin, cytokeratin and Vimentin, following manipulation of miR-379 expression. The expression levels of E-cadherin and cytokeratin were increased following transfection with pri-miR-379 when compared with the pcDNA3-NC, while the expression levels of Vimentin were significantly decreased under the same conditions (Fig. 1H). When transfected with ASO-miR-379, the expression levels of E-cadherin and cytokeratin were decreased compared with the ASO-NC, while the expression levels of Vimentin were significantly increased under the same conditions (Fig. 1H). This set of results demonstrated that miR-379 may act as a tumor suppressor, inhibiting the proliferation, migration and invasion of human NSCLC cells.

CHUK is a direct target of miR-379 in human NSCLC cells. To investigate the underlying mechanism of action of miR-379 in human NSCLC cells, the potential targets of miR-379 were

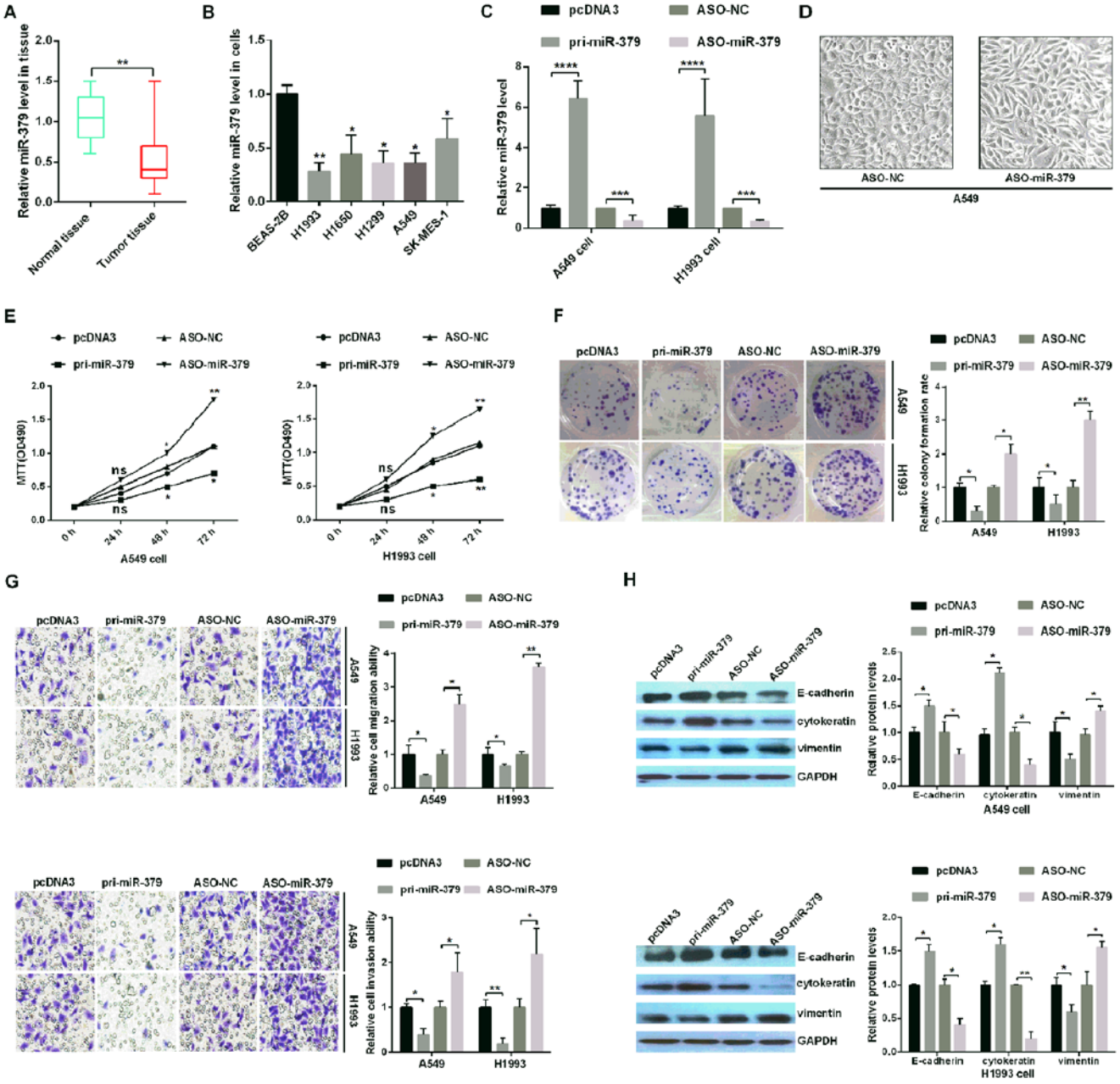

Figure 1. miR-379 inhibits tumorigenesis in human NSCLC tissues and cell lines. (A) The relative expression levels of miR-379 in tumor and paired normal lung tissues. (B) The expression of miR-379 across five NSCLC cell lines (H1993, H1650, H1299, SK-MES-1 and A549) and a non-tumorigenic human bronchial epithelial cell line (BEAS-2B) was analyzed by RT-qPCR. (C) The relative expression of miR-379 was analyzed by RT-qPCR in A549 and H1993 NSCLC cells transfected with pri-miR-379 (which upregulates miR-379), ASO-miR-379 (which downregulates miR-379) and control vectors (pcDNA3 and ASO-NC, respectively). (D) External cell morphology was evaluated using microscopy (magnification, x200). (E) Analysis of A549 and H1993 cell viability following transfection of the different plasmids was determined using an MTT assay. (F) The colony formation ability of A549 and H1993 cells following transfection with the different plasmids was determined using a colony formation assay. (G) miR-379 suppressed cell migration and cell invasion abilities, as demonstrated by the Transwell assays. Magnification, x10. (H) The protein levels of E-cadherin, cytokeratin and Vimentin were verified by western blotting assays in H1993 and A549 cells. All of the experiments were repeated at least four times. *P<0.05, **P<0.01, ***P<0.001 and ****P<0.0001, as indicated. miR, microRNA; NSCLC, non-small cell lung cancer; RT-qPCR, reverse transcription-quantitative PCR; ASO, antisense oligonucleotide; NC, negative control.

predicted using miRNA.org, TargetScan 7.1, miRbase and miRanda, and CHUK was identified as a potential target gene of miR-379 in subsequent experiments (Fig. 2A). To prove that miR-379 may directly target CHUK mRNA, EGFP reporter plasmids including the 3'UTR or the 3'UTR-mut of CHUK were constructed. The co-transfection of pri-miR-379 and wild type 3'UTR of CHUK significantly reduced the relative levels of EGFP activity, while the co-transfection of ASO-miR-379 and wild-type 3'UTR of CHUK significantly increased the relative EGFP activity (Fig. 2B). In addition, pri-miR-379 or ASO-miR-379 did not affect the relative EGFP activity levels when co-transfected with the mutant form of CHUK 3'UTR (Fig. 2C).

To further confirm the association between miR-379 and CHUK, the endogenous CHUK mRNA and protein levels in A549 and H1993 cells were evaluated following transfection with pri-miR-379 compared with ASO-miR-379 or the NCs pcDNA3 and ASO-NC. RT-qPCR and immunofluorescence assays demonstrated that pri-miR-379 significantly reduced

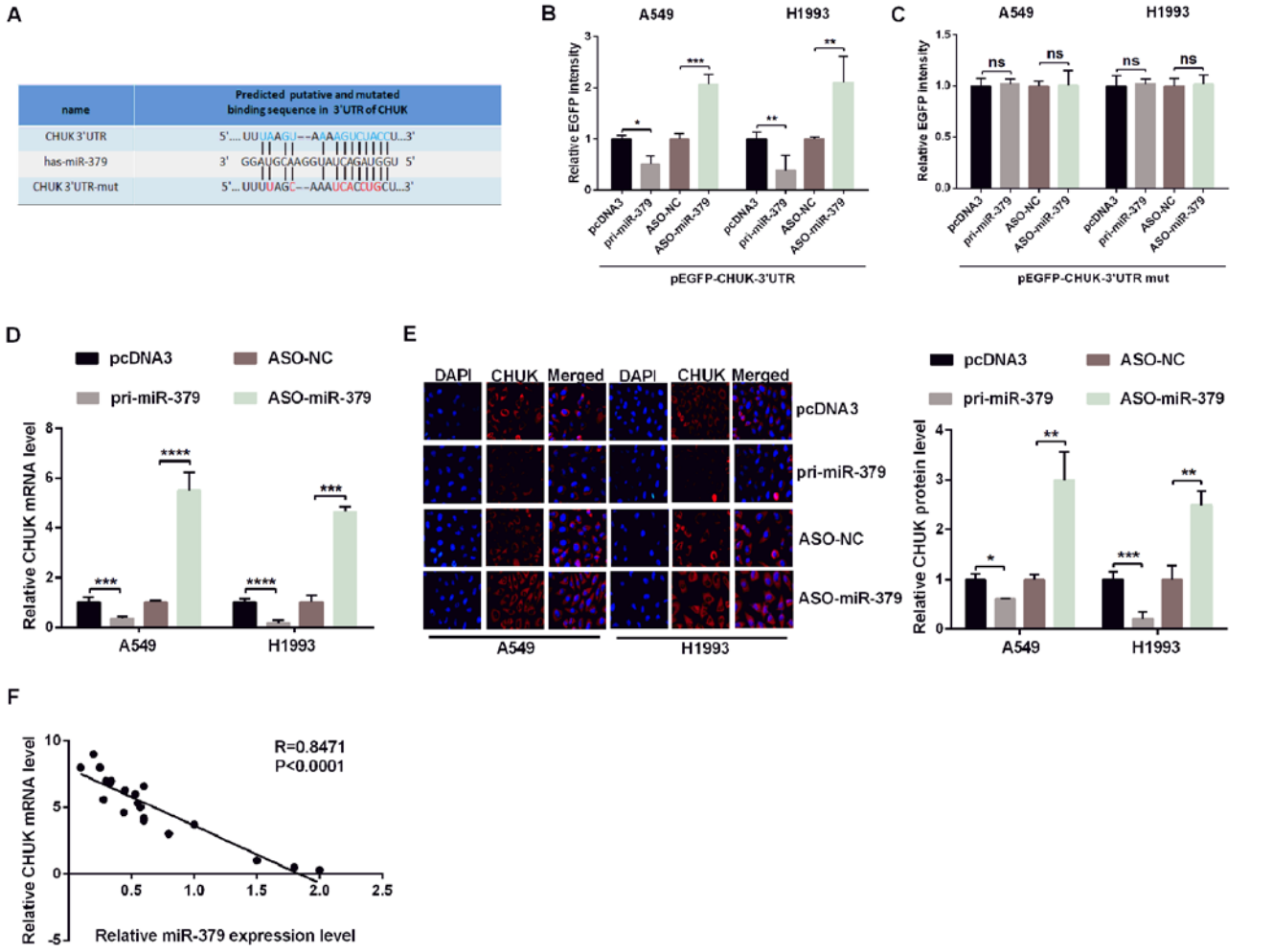

Figure 2. miR-379 directly targets CHUK in non-small cell lung cancer cells. (A) The predicted miR-379 binding sites were identified using TargetScan 7.1. CHUK was identified as a potential target mRNA, and its 3'UTR sequence, along with the mutated sequence are presented. A549 and H1993 cells were co-transfected with pri-miR-379 or ASO-miR-379 and with pcDNA3/EGFP-CHUK (B) 3'UTR or (C) 3'UTR-mut. EGFP intensity was measured by spectrophotometry, and the results revealed that CHUK is a direct target of miR-379 as shown by the increase in fluorescence in the presence of wild-type 3'UTR of CHUK. CHUK (D) mRNA levels and (E) protein expression in A549 and H1993 cells transfected with pri-miR-379 or ASO-miR-379 and the respective controls were determined by reverse transcription-quantitative PCR and immunofluorescence, respectively. (F) Correlation analysis of the expression data revealed a negative correlation between the expression of miR-379 and CHUK mRNA. All of the experiments were repeated at least four times. *P<0.05, **P<0.01, ***P<0.001 and ****P<0.0001, as indicated. miR, microRNA; CHUK, inhibitor of nuclear factor-κB kinase subunit α; UTR, untranslated region; mut, mutant; ASO, antisense oligonucleotide; EGFP, enhanced green fluorescent protein; NS, not significant; NC, negative control.

the expression of endogenous CHUK mRNA and protein (Fig. 2D and E). Additionally, as shown in Fig. 2F, the levels of CHUK mRNA are negatively correlated with the levels of miR-379. These results suggested that CHUK is a target gene of miR-379, and that it may be negatively regulated by miR-379 in human NSCLC cells.

CHUK functions as an oncogene in human NSCLC cells. To confirm the results obtained, the expression levels of CHUK mRNA were evaluated in 30 paired NSCLC tissues via RT-qPCR. The results revealed that the expression of CHUK mRNA was significantly upregulated in human NSCLC tissues compared with adjacent non-cancerous tissue samples (Fig. 3A). CHUK mRNA expression in the human NSCLC cell lines (H1993, H1650, H1299, SK-MES-1 and A549) and the BEAS-2B control cell line was also evaluated. This revealed that the expression levels of CHUK mRNA were markedly upregulated in the NSCLC cell lines compared with BEAS-2B (Fig. 3B). To investigate whether CHUK may affect NSCLC progression, H1993 and A549 cells were transfected with pcDNA3, pCHUK, pSilencer or shR-CHUK. RT-qPCR and western blotting assays demonstrated that the CHUCK mRNA and protein levels were upregulated with pCHUK and down-regulated with shR-CHUK in H1993 and A549 cells when compared with the respective controls (pcDNA3 and pSilencer, respectively; Fig. 3C and D). The overexpression of CHUK promoted cell proliferation, while the knockdown of CHUK had the opposite effect on both H1993 and A549 cells, as shown by the MTT and colony formation assays (Fig. 3E and F).

Regarding migration and invasion, H1993 and A549 cells transfected with pCHUK exhibited significantly greater invasion and migration capabilities in Transwell assays compared with pcDNA3-NC, while shR-CHUK significantly decreased invasion and migration capabilities of cells compared with pSilencer (Fig. 3G and H). The flow cytometry assay revealed that overexpression of CHUK may accelerate the cell cycle process, induce G1-S arrest and decrease the apoptotic rate in human NSCLC cells. On the other hand, the knockdown of CHUK reversed the

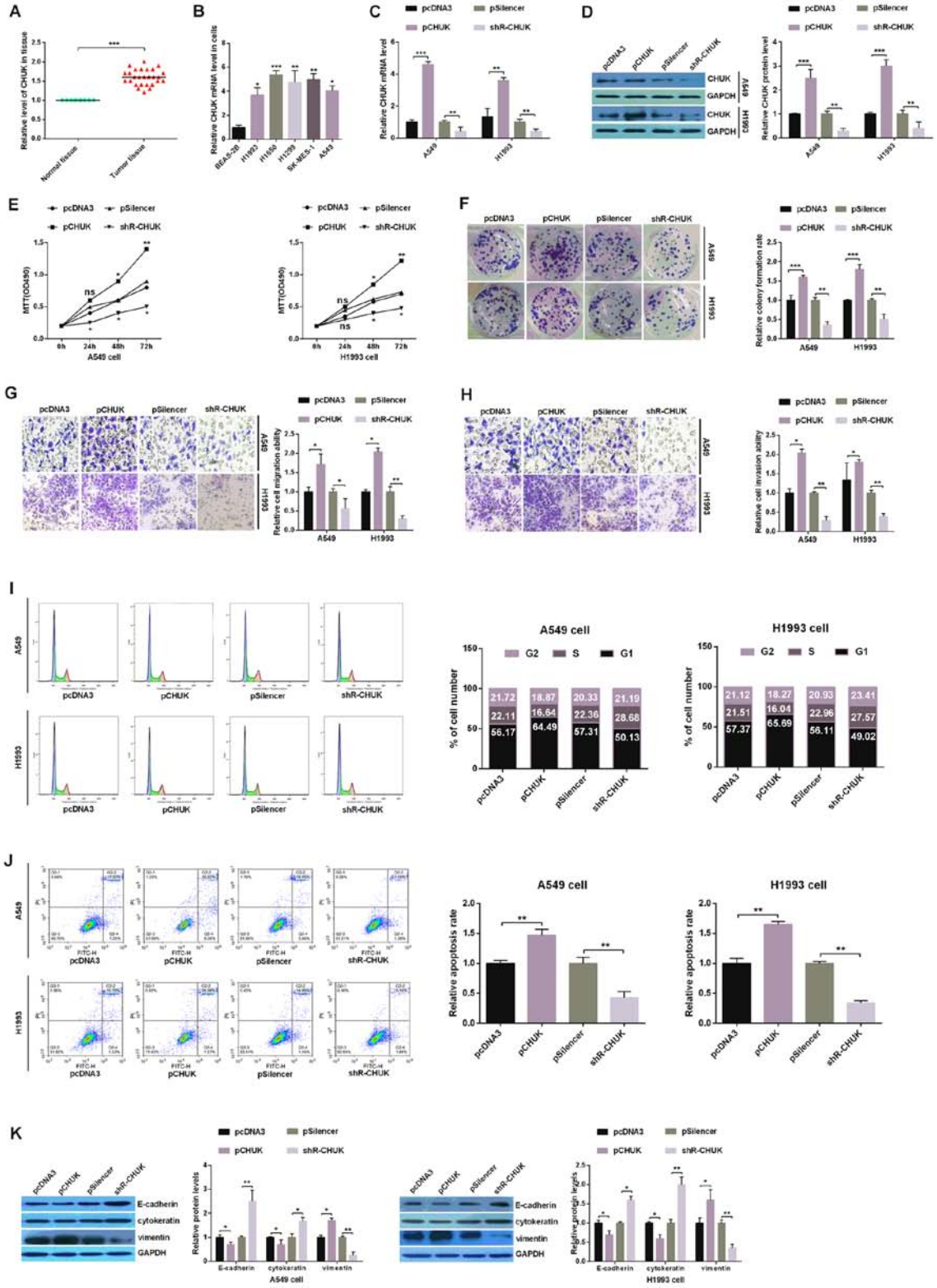

Figure 3. CHUK leads to the development of human NSCLC cells. (A) Relative expression levels of CHUK in tumor and paired normal lung tissues. (B) The relative expression of CHUK across five NSCLC cell lines (H1993, H1650, H1299, SK-MES-1 and A549) and a non-tumorigenic human bronchial epithelial cell line (BEAS-2B) was analyzed using RT-qPCR. A549 and H1993 cells were transfected with a CHUK overexpressing plasmid (pCHUK), shR-CHUK or an empty control plasmid (pcDNA3 or pSilencer, respectively). The efficiency of overexpression and knockdown of CHUK was demonstrated using (C) RT-qPCR and (D) western blotting. (E) Analysis of CHUK expression manipulation on the viability of A549 and H1993 cells was performed using an MTT assay. (F) The colony formation/proliferation ability of A549 and H1993 cells with both up- and downregulated levels of CHUK was determined using a colony formation assay. The (G) migration and (H) invasion abilities of transfected A549 and H1993 cells were determined using Transwell assays (magnification, x10). (I) Flow cytometry assay indicating the percentage of A549 and H1993 cells in different phases of the cell cycle following transfection with pCHUK or shR-CHUK and the respective controls. (J) The rates of apoptosis were measured using flow cytometry and by evaluating the levels of FITC and PI double staining. (K) The protein levels of E-cadherin, cytokeratin and Vimentin were analyzed using western blotting assays in H1993 and A549 cells. All of the experiments were repeated at least four times. *P<0.05, **P<0.01 and ***P<0.001, as indicated. miR, microRNA; NSCLC, non-small cell lung cancer; RT-qPCR, reverse transcription-quantitative PCR; CHUK, inhibitor of nuclear factor-κB kinase subunit α; shR, short hairpin RNA; FITC, fluorescein isothiocyanate; PI, propidium iodide.

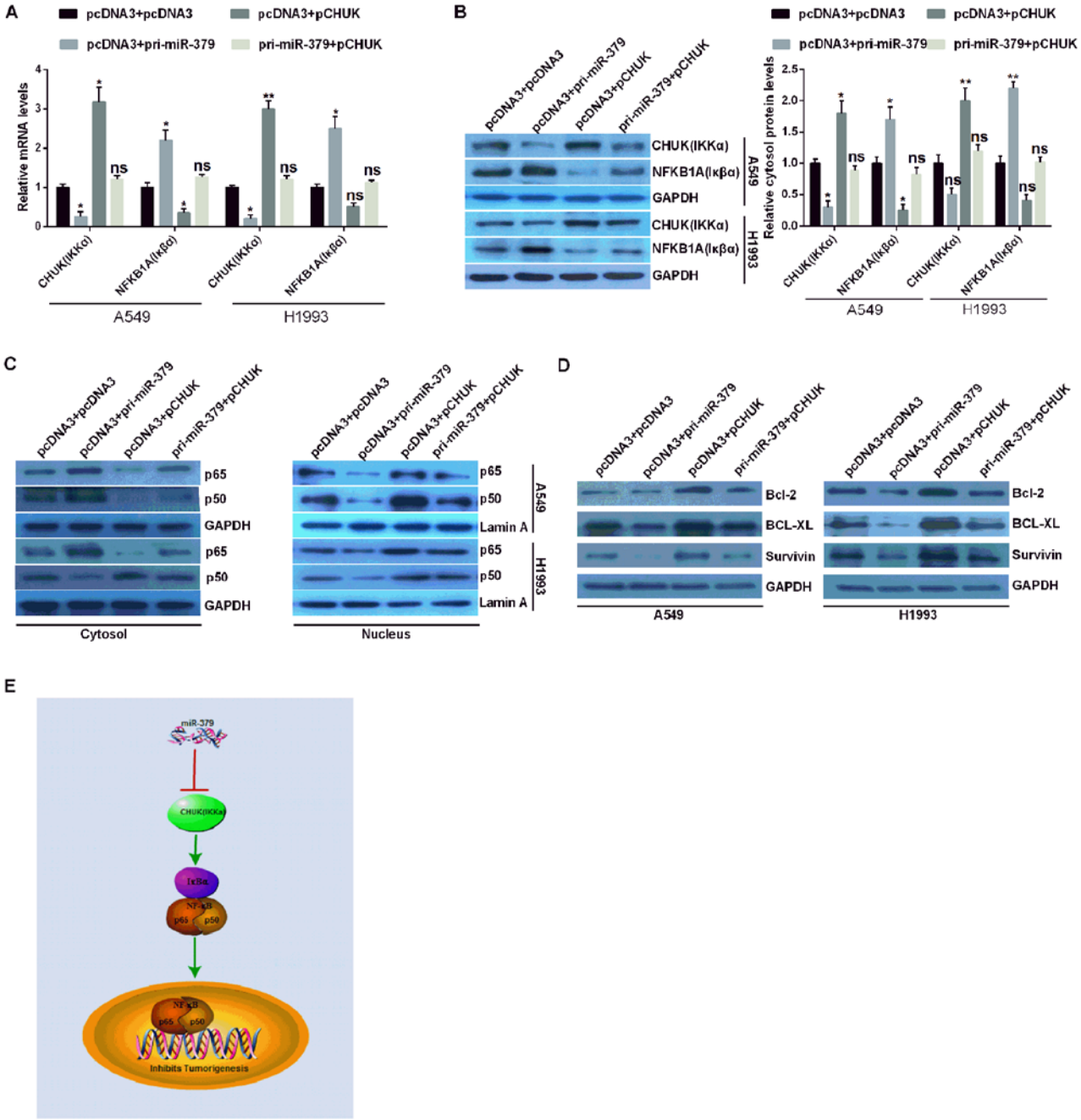

Figure 4. miR-379 inhibits the NF-κB signaling pathway in non-small cell lung cancer. (A) Reverse transcription-quantitative PCR and (B) western blotting were used to examine the levels of CHUK/IKKα and NFKBIA/Iκβα in A549 and H1993 cells. (C) Western blotting was used to examine the protein levels of NF-κB (p65 and p50) in the cytoplasmic and nuclear cellular fractions of A549 and H1993 cells. (D) Western blotting confirmed the protein levels of the downstream targets of NF-κB in A549 and H1993 cells, namely Bcl-2, Bcl-XL and survivin. (E) The proposed model indicating that miR-379 may suppress tumorigenesis by targeting CHUK and inhibiting the NF-κB signaling pathway. All of the experiments were repeated at least four times. *P<0.05 and **P<0.01, as indicated. miR, microRNA; CHUK/IKKα, inhibitor of nuclear factor-κB kinase subunit α; NF-κB, nuclear factor-κB; NFKBIA/Iκβα, NF-κB inhibitor α; NS, not significant.

above results (Fig. 3I and J). Lastly, the levels of E-cadherin and cytokeratin were observed to be downregulated, while Vimentin was upregulated in cells that overexpressed CHUK. Conversely, the knockdown of CHUK promoted the expression of E-cadherin and cytokeratin, while suppressing the expression of Vimentin (Fig. 3K). These results suggest that CHUK may function as an oncogene in human NSCLC cells.

miR-379 inhibits the NF-κB pathway via the downregulation of CHUK in NSCLC. In order to confirm whether miR-379 affected the NF-κB signaling pathway in NSCLC cells, the expression levels of the CHUK/IKKα genes and NFKBIA (Iκβα) were analyzed via RT-qPCR and western blotting assays. The results demonstrated that NFKBIA (Iκβα) was suppressed following CHUK (IKKα) overexpression, but promoted following CHUK (IKKα) downregulation in the context of miR-379 overexpression (Fig. 4A and B). p65 (NF-κB3) and p50 (NF-κB1) are heterodimers identified as constituting members of NF-κB (18). Therefore, the nuclear distribution of p65 and p50 may have increased in pCHUK-transfected cells,

and decreased in pri-miR-379-transfected cells. The distribution levels of p65 and p50 in the nucleus did not change in A549 and H1993 cells co-transfected with pri-miR-379 and pCHUK (Fig. 4C). However, under the same conditions, the expression of p65 and p50 in the cytoplasm is opposite to that of the nucleus (Fig. 4C). These results demonstrated that CHUK may increase the expression of p65 and p50 in cell nuclei.

Therefore, it was hypothesized that CHUK may activate NF-κB in NSCLC cells. To clarify this hypothesis, the expression levels of Bcl-2, BCL-XL and survivin were detected. The expression levels of these genes were higher in NSCLC cells overexpressing CHUK and lower in NSCLC expressing miR-379. The expression levels of Bcl-2, BCL-XL and survivin were similar in miR-379 and CHUK co-transfected NSCLC cells compared with those in pcDNA3 + pcDNA3 co-transfected NSCLC cells (Fig. 4D). These results suggested that miR-379 may inhibit tumorigenesis by directly targeting CHUK 3'UTR, inhibiting CHUK expression, and potentially suppressing the NF-κB signaling pathway in NSCLC (Fig. 4E).

Discussion

NSCLC is one of the most common types of tumors and has a high mortality rate (19). The occurrence of NSCLC is a multi-stage process characterized by significant changes in gene expression and in the physiological structure of the lung tissue (20). Alterations in gene expression may involve the inactivation of tumor suppressor genes or the activation of oncogenes, which causes further abnormalities in gene expression (21). Although research on NSCLC has led to the development of several therapeutic approaches, including radiation therapy, chemotherapy and surgical resection, NSCLC remains difficult to treat and has a poor prognosis (22). In order to fully discern the progression of NSCLC, a deeper understanding of the associated gene expression profiles and related biological mechanisms is required to improve current treatments.

Previous studies have shown that miRs have crucial roles during tumorigenesis (23-29), and that miR-379 is downregulated in many types of cancer. For example, Xie *et al* (30) reported that miR-379 was downregulated in human osteosarcoma specimens and cell lines, that miR-379 overexpression inhibited cell proliferation and colony formation and that it promoted a G0/G1 cell cycle arrest in human osteosarcoma cells. In addition, Li *et al* (31) reported that miR-379 inhibited vascular smooth muscle cell function and survival by targeting insulin-like growth factor-1 through the activation of extracellular signaling pathways in these cells. Furthermore, Chen *et al* (32) reported that miR-379-5p may repress cell invasion and metastasis, promote apoptosis and inhibit cell cycle progression by targeting the protein tyrosine kinase 2/AKT serine/threonine kinase signaling pathway in hepatocellular carcinoma. These studies suggested that miR-379 may have important functions in various types of cancer, and may constitute as a therapeutic target in the treatment of these diseases. In the present study, it was demonstrated that miR-379 is significantly downregulated in NSCLC tissues and cell lines. The overexpression of miR-379 may have significantly inhibited growth, migration and invasion, promoted apoptosis, and arrested the cell cycle of NSCLC cells *in vitro* by reducing the expression levels of Vimentin and promoting the expression of cytokeratin and E-cadherin. Overall, the results suggested that this miR may serve as a cancer gene suppressor in human NSCLC cells. In addition, overexpression of miR-379 may inactivate the NF-κB signaling pathway in NSCLC cells.

miRs serve an important role across a variety of biological processes, including cancer, via complementary binding with the 3'UTR of their target genes (33). In the present study, bioinformatic analysis was used to predict the target genes of miR-379, and CHUK was chosen as a potential target. Furthermore, the expression level of CHUK mRNA and protein was distinctly increased in the H1993, H1650, H1299, SK-MES-1 and A549 cell lines, which was inversely correlated with the levels of miR-379 in NSCLC cells. In addition, a EGFP reporter assay revealed that miR-379 directly targeted the 3'UTR of the CHUK mRNA in A549 and H1993 cells. RT-qPCR and western blot assays further demonstrated that the overexpression of miR-379 was associated with a significant decrease in the expression of CHUK and that the knockdown of miR-379 increased the expression of CHUK in both A549 and H1993 cells.

The NF-κB signaling pathway serves important roles in a number of biological processes, including immunity, inflammatory and apoptotic responses (34). The activation of the NF-κB pathway is also involved in the pathogenesis of a variety of diseases, including many types of human cancers. Notably, the activation of NF-κB may also induce the expression of anti-apoptotic genes in germ cells, which may in turn attenuate germ cell apoptosis (35). The activation of NF-κB is also involved in the cisplatin resistance of various types of cancer (36,37). Naidu *et al* (38) reported that platelet-derived growth factor receptor-modulated miR-23b and miR-125a-5p may inhibit lung tumorigenesis by targeting multiple components of the KRAS and NF-κB pathways. All of these studies confirmed that CHUK may be involved in tumorigenesis; however, the function of CHUK in NSCLC remained unclear. The results of the present study confirmed that the expression levels of CHUK, at both the mRNA and protein levels, were upregulated in NSCLC cell lines, and the overexpression of CHUK may have enhanced cell viability, colony formation ability and the EMT process in NSCLC cells. Furthermore, ectopic CHUK expression may have activated the NF-κB signaling pathway in NSCLC cells.

The present study demonstrated that the downregulation of miR-379 in NSCLC tissues and cell lines is a common phenomenon, and that miR-379 may serve an important role in regulating the growth, migration and invasion of human NSCLC cells by promoting EMT. In addition, miR-379 inhibited the expression of CHUK by directly targeting the 3'-UTR of CHUK mRNA and miR-379 may have inhibited the activation of the NF-κB signaling pathway by regulating CHUK in NSCLC cells. In conclusion, the results of the present study may have provided novel insights into NSCLC tumorigenesis, and provided a potential new therapeutic target for the treatment for NSCLC.

Acknowledgements

Not applicable.

Funding

No funding was received.

Availability of data and materials

The datasets used and/or analyzed during the current study are available from the corresponding author on reasonable request.

Authors' contributions

BL, ZW and SC performed the experiments, analyzed the data and wrote the manuscript. JZ designed and supervised the study and wrote the manuscript. LD, YY and ZY assisted with data collection and analysis, and wrote the manuscript.

Ethics approval and consent to participate

All participants provided written informed consent. The present study was approved by the Ethical Oversight Committee of Department of Respiratory and Critical Care Medicine, Tianjin Chest Hospital (Tianjin, China).

Patient consent for publication

Not applicable.

Competing interests

The authors declare that they have no competing interests.

References

1. Siegel RL, Miller KD and Jemal A: Cancer statistics, 2016. CA Cancer J Clin 66: 7-30, 2016.
2. Cheng H, Shcherba M, Kandavelou K, Liang Y, Liu H and Perez-Soler R: Emerging drugs for squamous cell lung cancer. Expert Opin Emerg Drugs 20: 149-160, 2015.
3. Karlsen TA, De Souza GA, Degaard B, Engebretsen L and Brinchmann JE: MicroRNA-140 inhibits inflammation and stimulates chondrogenesis in a model of interleukin 1β-induced osteoarthritis. Mol Ther Nucleic Acids 5: e373, 2016.
4. Yin J, Wang M, Jin C and Qi Q: MiR-101 sensitizes A549 NSCLC cell line to CDDP by activating caspase 3-dependent apoptosis. Oncol Lett 7: 461-465, 2014.
5. Zinner R, Visseren-Grul C, Spigel DR and Obasaju C: Pemetrexed clinical studies in performance status 2 patients with non-small cell lung cancer (review). Int J Oncol 48: 13-27, 2016.
6. Ameres SL and Zamore PD: Diversifying microRNA sequence and function. Nat Rev Mol Cell Biol 14: 475-488, 2013.
7. Bartel DP: MicroRNAs: Genomics, biogenesis, mechanism, and function. Cell 116: 281-297, 2004.
8. Thayanithy V, Sarver AL, Kartha RV, Li L, Angstadt AY, Breen M, Steer CJ, Modiano JF and Subramanian S: Perturbation of 14q32 miRNAs-cMYC gene network in osteosarcoma. Bone 50: 171-181, 2012.
9. Bartel DP: MicroRNAs: Target recognition and regulatory functions. Cell 136: 215-233, 2009.
10. Makeyev EV and Maniatis T: Multilevel regulation of gene expression by microRNAs. Science 319: 1789-1790, 2008.
11. Yu N, Zhang Q, Liu Q, Yang J and Zhang S: A meta-analysis: microRNAs' prognostic function in patients with nonsmall cell lung cancer. Cancer Med 6: 2098-2105, 2017.
12. Zhang K, Han X, Zhang Z, Zheng L, Hu Z, Yao Q, Cui H, Shu G, Si M, Li C, *et al*: The liver-enriched lnc-LFAR1 promotes liver fibrosis by activating TGFβ and Notch pathways. Nat Commun 8: 144, 2017.
13. Legras A, Pécuchet N, Imbeaud S, Pallier K, Didelot A, Roussel H, Gibault L, Fabre E, Le Pimpec-Barthes F, Laurent-Puig P and Blons H: Epithelial-to-mesenchymal transition and microRNAs in lung cancer. Cancers (Basel) 9: pii: E101, 2017.
14. Wang M, Meng B, Liu Y, Yu J and Chen Q: MiR-124 inhibits growth and enhances radiation-induced apoptosis in non-small cell lung cancer by inhibiting STAT3. Cell Physiol Biochem 44: 2017-2028, 2017.
15. Liu J, Bian T, Feng J, Qian L, Zhang J, Jiang D, Zhang Q, Li X, Liu Y and Shi J: miR-335 inhibited cell proliferation of lung cancer cells by target Tra2β. Cancer Sci 109: 289-296, 2018.
16. Xue X, Fei X, Hou W, Zhang Y, Liu L and Hu R: miR-342-3p suppresses cell proliferation and migration by targeting AGR2 in non-small cell lung cancer. Cancer Lett 412: 170-178, 2018.
17. Livak KJ and Schmittgen TD: Analysis of relative gene expression data using real-time quantitative PCR and the 2(-Delta Delta C(T)) method. Methods 25: 402-408, 2001.
18. Le F, Zhang JY, Liu W, Huang XM and Luo WZ: The levels of NF-κB p50 and NF-κB p65 play a role in thyroid carcinoma malignancy in vivo. J Int Med Res 46: 4092-4099, 2018.
19. Liu XH, Liu ZL, Sun M, Liu J, Wang ZX and De W: The long non-coding RNA HOTAIR indicates a poor prognosis and promotes metastasis in non-small cell lung cancer. BMC Cancer 13: 464, 2013.
20. Chen X, Chen S, Hang W, Huang H and Ma H: MiR-95 induces proliferation and chemo- or radioresistance through directly targeting sorting nexin1 (SNX1) in non-small cell lung cancer. Biomed Pharmacother 68: 589-595, 2014.
21. Zhang Y, Zhao Y, Sun S, Liu Z, Zhang Y and Jiao S: Overexpression of microRNA-221 is associated with poor prognosis in non-small cell lung cancer patients. Tumour Biol 37: 10155-10160, 2016.
22. Sun S, Schiller JH, Spinola M and Minna JD: New molecularly targeted therapies for lung cancer. J Clin Invest 117: 2740-2750, 2007.
23. Sun C, Liu Z, Li S, Yang C, Xue R, Xi Y, Wang L, Wang S, He Q, Huang J, *et al*: Down-regulation of c-Met and Bcl2 by microRNA-206, activates apoptosis, and inhibits tumor cell proliferation, migration and colony formation. Oncotarget 6: 25533-25574, 2015.
24. Bier A, Giladi N, Kronfeld N, Lee HK, Cazacu S, Finniss S, Xiang C, Poisson L, Decarvalho AC, Slavin S, *et al*: MicroRNA-137 is downregulated in glioblastoma and inhibits the stemness of glioma stem cells by targeting RTVP-1. Oncotarget 4: 665-676, 2013.
25. Sun C, Huang C, Li S, Yang C, Xi Y, Wang L, Zhang F, Fu Y and Li D: Hsa-miR-326 targets CCND1 and inhibits non-small cell lung cancer development. Oncotarget 7: 8341-8359, 2016.
26. Sun C, Li S, Zhang F, Xi Y, Wang L, Bi Y and Li D: Long non-coding RNA NEAT1 promotes non-small cell lung cancer progression through regulation of miR-377-3p-E2F3 pathway. Oncotarget 7: 51784-51814, 2016.
27. Sun CC, Li SJ, Zhang F, Zhang YD, Zuo ZY, Xi YY, Wang L and Li DJ: The novel miR-9600 suppresses tumor progression and promotes paclitaxel sensitivity in non-small-cell lung cancer through altering STAT3 expression. Mol Ther Nucleic Acids 5: e387, 2016.
28. Zhang C, Liu J, Wang X, Wu R, Lin M, Laddha SV, Yang Q, Chan CS and Feng Z: MicroRNA-339-5p inhibits colorectal tumorigenesis through regulation of the MDM2/p53 signaling. Oncotarget 5: 9106-9117, 2014.
29. Xi Y, Wang L, Sun C, Yang C, Zhang F and Li D: The novel miR-9501 inhibits cell proliferation, migration and activates apoptosis in non-small cell lung cancer. Med Oncol 33: 124, 2016.
30. Xie X, Li YS, Xiao WF, Deng ZH, He HB, Liu Q and Luo W: MicroRNA-379 inhibits the proliferation, migration and invasion of human osteosarcoma cells by targetting EIF4G2. Biosci Rep 37: pii: BSR20160542, 2017.
31. Li K, Wang Y, Zhang A, Liu B and Jia L: miR-379 inhibits cell proliferation, invasion, and migration of vascular smooth muscle cells by targeting insulin-like factor-1. Yonsei Med J 58: 234-240, 2017.
32. Chen JS, Li HS, Huang JQ, Dong SH, Huang ZJ, Yi W, Zhan GF, Feng JT, Sun JC and Huang XH: MicroRNA-379-5p inhibits tumor invasion and metastasis by targeting FAK/AKT signaling in hepatocellular carcinoma. Cancer Lett 375: 73-83, 2016.
33. Majidinia M, Aghazadeh J, Jahanban-Esfahlani R and Yousefi B: The roles of Wnt/β-catenin pathway in tissue development and regenerative medicine. J Cell Physiol 233: 5598-5612, 2017.
34. Perkins ND: Integrating cell-signalling pathways with NF-kappaB and IKK function. Nat Rev Mol Cell Biol 8: 49-62, 2007.

35. Wright A, Reiley WW, Chang M, Jin W, Lee AJ, Zhang M and Sun SC: Regulation of early wave of germ cell apoptosis and spermatogenesis by deubiquitinating enzyme CYLD. Dev Cell 13: 705-716, 2007.
36. Mabuchi S, Ohmichi M, Nishio Y, Hayasaka T, Kimura A, Ohta T, Saito M, Kawagoe J, Takahashi K, Yada-Hashimoto N, *et al*: Inhibition of NFkappaB increases the efficacy of cisplatin in in vitro and in vivo ovarian cancer models. J Biol Chem 279: 23477-23485, 2004.
37. Li Y, Ahmed F, Ali S, Philip PA, Kucuk O and Sarkar FH: Inactivation of nuclear factor KB by soy isoflavone genistein contributes to increased apoptosis induced by chemotherapeutic agents in human cancer cells. Cancer Res 65: 6934-6942, 2005.
38. Naidu S, Shi L, Magee P, Middleton JD, Laganá A, Sahoo S, Leong HS, Galvin M, Frese K, Dive C, *et al*: PDGFR-modulated miR-23b cluster and miR-125a-5p suppress lung tumorigenesis by targeting multiple components of KRAS and NF-κB pathways. Sci Rep 7: 15441, 2017.